Journal of Thermal Science Vol.27, No.2 (2018) 135−145

https://doi.org/10.1007/s11630-018-0994-3 **Article ID: 1003-2169(2018)02-0135-11**

Numerical Investigations of the Influence of Unsteady Vane Trailing Edge Shock Wave on Film Cooling Effectiveness of Rotor Blade Leading Edge

WANG Yufeng, CAI Le, WANG Songtao, ZHOU Xun

Engine Aerodynamics Research Centre Harbin Institute of Technology Harbin 150001, China

Unsteady numerical simulations of a high-load transonic turbine stage have been carried out to study the influences of vane trailing edge outer-extending shockwave on rotor blade leading edge film cooling performance. The turbine stage used in this paper is composed of a vane section and a rotor one which are both near the root section of a transonic high-load turbine stage. The Mach number is 0.94 at vane outlet, and the relative Mach number is above 1.10 at rotor outlet. Various positions and oblique angles of film cooling holes were investigated in this research. Results show that the cooling efficiency on the blade surface of rotor near leading edge is significantly affected by vane trailing edge outer-extending shockwave in some cases. In the cases that film holes are close to leading edge, cooling performance suffers more from the sweeping vane trailing edge outer-extending shockwave. In addition, coolant flow ejected from oblique film holes is harder to separate from the blade surface of rotor, and can cover more blade area even under the effects of sweeping vane trailing edge shockwave. As a result, oblique film holes can provide better film cooling performance than vertical film holes do near the leading edge on turbine blade which is swept by shockwaves.

Keywords: transonic turbine, trailing edge shock wave, film cooling, unsteady simulation

Introduction

The inlet temperature of turbine used in aircraft engine has been constantly improved to enhance thrust, increase efficiency and reduce SFC. Limited to heat resisting property of turbomachinery blade material, film cooling and other cooling methods should be applied to the design of turbine blade so that it can withstand the high temperature gas. The leading edge is the first part to contact the high temperature gas on a turbine blade, which is in the severest operating condition. Therefore, leading edge cooling is widely concerned. Besides, the unsteady characteristic caused by relative rotation of upstream vane and downstream rotor also has a significant influence on the flow structures in the passage of rotor, and that influence even reflects in the differences of total parameters [1]. In transonic turbine, gas flow near the leading edge of rotor blade will be affected by upstream vane trailing edge outer-extending shockwave. The sweeping outer-extending shockwave can cause the pressure fluctuations, the changes of boundary layer thickness, and the boundary layer separations, which not only increases blade surface viscosity loss [2], but also reduces film cooling effectiveness near the leading edge of rotor blade [3]. Therefore, it is necessary to research the effects of vane trailing edge outer-extending shockwave on film cooling effectiveness near the leading edge of rotor blade in a transonic turbine stage, which can provide a refer. ence for film cooling design at leading edge of transonic turbine stage.

Received: October 17, 2017 WANG Yufeng: PhD candidate E-mail: wangyflp@126.com
This research is supported by National Natural Science Foundation of China , Grant No. 51421063.

Nomenclature		Abbreviations, Subscripts and Superscripts	
t	Pitch [mm]	SS	Suction side
c	Chord length [mm]	PS	Pressure side
l	Length [mm]	LE	Leading edge
d	Diameter of film hole [mm]	0p	Vane inlet
S	Blade profile curve length [mm]	1p	Vane outlet
h	Blade height [mm]	2p	Rotor outlet
γ	Stagger angle [°]	1	Vane
α	Blade metal angle (stator) [°]	2	Rotor
β	Blade metal angle (rotor) [°]	c	Coolant
θ	Angle between film hole axis and blade surface [°]	ax	Axial direction
T	Temperature [K]	H	Film hole
T	Period [s]	∞	Incoming flow
Ma	Mach number [-]	*	Total conditions
η	Film cooling efficiency [-]		

There have been many researches to investigate film cooling effectiveness in the flow passages of transonic turbine. Adami et al studied the effects of unsteady interaction on film cooling effectiveness by numerical calculation methods [4]. They pointed out that the unsteady interaction between upstream vane and downstream rotor can affect the mixture of gas and coolant downstream of film cooling holes and cause boundary layer separations, which results in the coolant coverage on downstream blade surface being affected. Experimental studies were performed to investigate the effects of interaction between vane and rotor on film cooling effectiveness in a linear turbine stage cascade [5, 6]. They found that because of the vane/blade interaction, heat transfer coefficient on downstream blade surface fluctuates obviously in the turbine stage even without coolant ejection. Therefore, this kind of interaction can produce a remarkable influence on film cooling effectiveness. Li et al pointed out that the vane/blade interaction impacts inlet angle of downstream blade passage and then affects its cooling effectiveness indirectly [7]. Rigby et al and Zhou et al investigated the effects of unsteady interaction on the film cooling performance at the leading edge of downstream blade. Their results showed that unsteady trailing edge shockwave can influence coolant flow near leading edge of downstream blade [8, 9].

Based on the previous work, it is obviously that the vane/blade unsteady interaction in a turbine stage can have a profound influence on the film cooling performance on downstream blade surface. In transonic turbine stage, the outer-extending shockwave at the trailing edge of the vane will cause the unsteady interaction to be more complex, which is rarely investigated before. In this study, film cooling holes are placed at different locations near leading edge to find out how unsteady trailing edge outer-extending shockwave affects leading edge cooling effectiveness, which can provide a reference for transonic turbine blade leading edge cooling design.

Model and Numerical Method

Turbine stage cascade used for this study

The turbine stage cascade studied in this article is the root section of a high-load transonic high pressure turbine stage, as shown in Fig.1. Table.1 shows the basic aerodynamic and geometry parameters of this turbine stage.

Two round film cooling holes are placed along radial direction near the leading edge of rotor blade. The radial positions of film holes are 25% span and 75% span. The chordwise position of the two film holes is determined by length of the blade profile curve between leading edge point and center point of the film hole on blade surface, which is shown in Fig.2. Basic geometry parameters are shown in Table 2. For the case in which film holes are

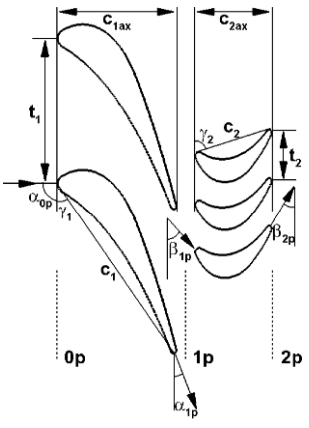

Fig. 1 Turbine stage blade profile configuration

Table 1 Basic aerodynamic and geometry parameters of the turbine stage

Parameter		Value
	γ_1 /(°)	34.24
	α_{0p} /(°)	90.00
	α_{1p} /(°)	15.14
VANE	t_1/(mm)	63.25
	c_1 /(mm)	91.85
	h/(mm)	8.00
	Ma_1	0.94
	γ_2 /(°)	72.08
	β_{1p} /(°)	41.22
	β_{2p} /(°)	23.57
ROTOR	t_2/(mm)	21.08
	c_2 /(mm)	35.05
	h/(mm)	8.00
	Ma_2	1.10

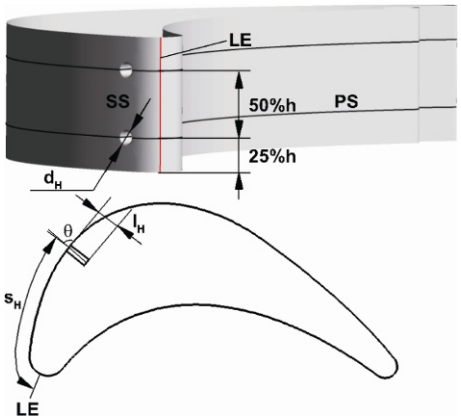

Fig. 2 Schematic of film hole

Table 2 Geometry parameters of film cooling holes

Parameter	Value
θ/(°)	90.00,30.00
d_H /(mm)	0.80
l_H /(mm)	1.60
S_H/S_{ss} /(-)	0.00,0.05,0.10,0.15,0.20

located at leading edge, the axis of film hole is perpendicular to the blade surface. In other cases, both θ=90° and θ=30° conditions are investigated.

Grids and boundary conditions

The number of rotor blade is three times of that of vane. The meshing process was completed using an automatic air-cooled turbine blade mesh-generating program [10], which had already been verified reasonable and frequently used [11-13]. As shown in Fig.3, the grids in vane and rotor domains are all structured and each of them has an O-4H topological structure. Total grid number of all computational domains is 3.83 million and each of the rotor domain has a grid number of 0.79 million. The thickness of the first layer grid cells on blade surface is limited under 1×10^{-6} m so that the flow into boundary layers can be simulated accurately.

The working substance at inlet of vane computational domain is fuel gas, which has a total pressure of 2078kPa and a total temperature of 1600K. The averaged static pressure at outlet of the rotor domain is 571kPa. Coolant working substance is ideal gas. The hub and shroud were both set as adiabatic slip wall while other solid walls were adiabatic no slip walls. Velocity boundary condition was set at the inlet of film cooling holes to guarantee that the blow ratio is around 1.0.

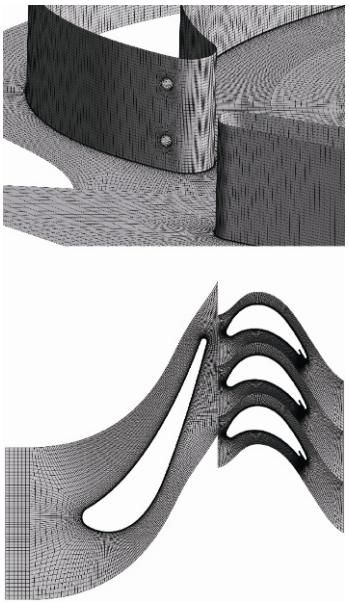

Fig. 3 Grids of computational domain

Grid resolution study

Grid resolution study was conducted in the case of S_H/S_{ss} =0.10 and θ=90° before the detailed calculations in all cases being carried out. Four sets of grids in different levels were generated in this study. The grid numbers corresponding to each set of grid are shown in Table 3.

Table 3 Grid numbers of each set of grid (million)

	VANE	ROTOR	TOTAL
m30w	0.51	0.50	2.01
m15w	0.65	0.64	2.59
m00w	0.79	0.79	3.83
p30w	1.11	1.09	4.36

Fig.4 shows the cooling efficiency distributions on suction side at 25% rotor span in steady result and time averaged unsteady one. According to Fig.4a, it is easy to see that the cooling efficiencies in all the cases are nearly the same. The maximum deviation of cooling efficiency between those cases is not more than 0.01. In unsteady time-averaged results, as shown in Fig.4b, the distributions of cooling efficiencies in m30w and m15w cases are relatively far from those in m00w and p30w cases. The result in m00w case is very close to that in p30w case, which means that in this study, the grid level in m00w case has the sufficient grid resolution. So the grid level in m00w case (0.79 million in vane computational domain and 0.79 in each of rotor computational domains) was chosen for the reasons of insuring the accuracy and saving the computing resource cost.

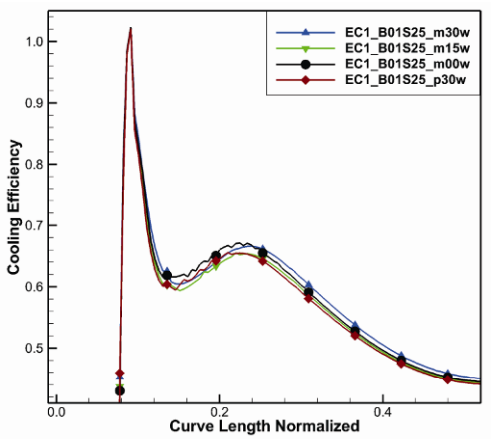

Fig. 4 Cooling efficiency distributions at 25% span on suction side

Numerical method

CFX of ANSYS software package is used in this study to solve steady Reynolds-averaged Navier-Stokes equations. SST turbulence model was selected. The reason is that the numerical simulation results based on SST model are relatively in good agreement with the experimental results in air-cooled turbine blades [14-17], which means that the turbulence model used in this paper is reasonable. In this study, the computational period was set as the elapsed time for a rotor blade to rotate a pitch. Every computational period is divided into 60 physical time steps.

Results and Analysis

Structure and movement of vane shockwave

The rotor blade surface cooling efficiency distributions at 25% and 50% spans in the case with leading edge coolant ejection are shown in Fig.5. Cooling efficiency is defined as shown in formula (1):

$$\eta = \frac{T_\infty^* - T}{T_\infty^* - T_c^*} \tag{1}$$

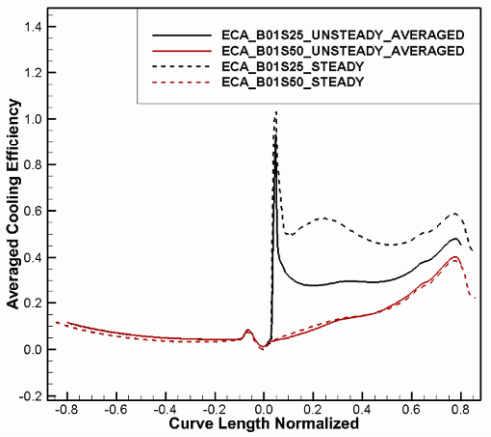

Fig. 5 Rotor blade surface cooling efficiency distributions at 25% and 50% spans in the case with leading edge cooling injection S_H/S_{SS}=0.05

In Fig.5 the horizontal axis represents for the normalized blade profile curve length. Zero represents leading edge position. The positive half axis and the negative one stand for suction side and pressure side, respectively. Solid lines and dashed ones represent for averaged unsteady results and steady ones, respectively. As shown in this figure, at 50% span, the distribution of unsteady time-averaged cooling efficiency agrees well with that of steady result, where there is no film holes. However, when it comes to 25% span, those two distributions from different results show a significant difference. Thus it can be seen that in high load transonic turbine stages, vane/blade interruption and the unsteady vane trailing edge shockwave sweeping both have a significant effect on the distribution of film cooling efficiency on rotor blade surface, which is in accordance with the conclusions in ref-

erences [7, 18, 19]. In addition, according to cooling efficiency contours on the suction sides, as shown in Fig.6, we can see that not only the numeric value but also the distribution regularity have a lot of differences in cooling efficiency distributions, including the spanwise distributions and changes of value monotony.

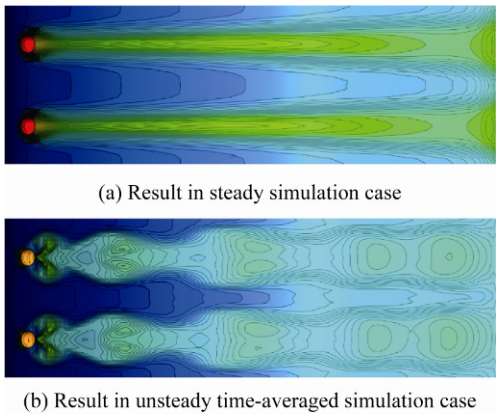

(a) Result in steady simulation case

(b) Result in unsteady time-averaged simulation case

Fig. 6 Suction side cooling efficiency contours in the case with S_H/S_{SS} =0.00

Fig.7 shows the Mach contour at 25% span near the leading edge of rotor blade at a certain moment. It can be seen that the outer-extending shockwave at vane trailing edge can reach rotor blade surface at this moment. We can denote the contact point of blade surface and shockwave as point A. As the rotor blade turns, point A travels along blade profile from suction side to leading edge. After reaching leading edge, point A begins to travel towards pressure side for a very short distance. Then, it will detach from the blade surface until the adjacent rotor blade turns to a specific position where shockwave can reach blade suction side again. This process cycles with the rotation of rotor blade. Therefore, the outer-extending shockwave at vane trailing edge can affect flow field near rotor blade leading edge at certain moments, including pressure, temperature and other parameters on blade surface.

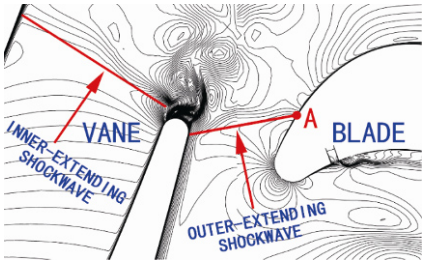

Fig. 7 The shockwave structure at vane trailing edge

Film cooling performance: case S_H/S_{SS} =0.00

Fig.8 shows the cooling efficiency distribution at 25% rotor span in the case with S_H/S_{SS}=0.00. It can be seen that the region with high film cooling efficiency appears on suction side and pressure side periodically.

Fig.9 shows the gas and coolant streamlines at several moments with the background of local Mach contour. Red lines and black ones represent for gas and coolant, respectively. At the moment of t=0.0556T, nearly all of the coolant flows towards the suction side under the influence of incoming gas flow direction. At this moment, the coolant cannot cover pressure side of rotor blade. At the moment of t=0.1944T, coolant begins to flow towards the pressure side and its flow rate becomes higher over time. Consequently, the high film cooling efficiency zone begins to appear on the pressure side. When the time reaches t=0.6111T, almost all of the coolant flows towards the pressure side and film cooling efficiency on the pressure side was clearly higher than that on the suction side at this moment. From then on, the coolant begins to flow towards the suction side again. At the moment of t=0.8889T, both the suction side and the pressure side are covered with coolant flow at 25% span.

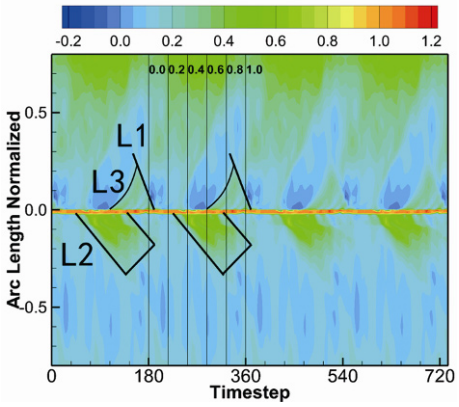

Fig. 8 Cooling efficiency contour at 25% rotor span in the case with S_H/S_{SS} =0.00

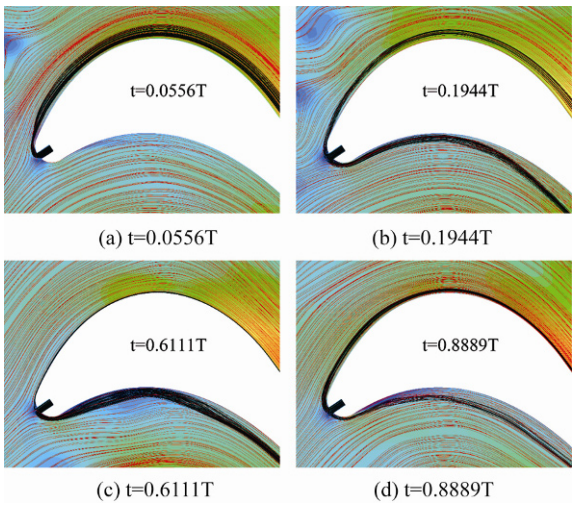

(a) t=0.0556T (b) t=0.1944T

(c) t=0.6111T (d) t=0.8889T

Fig. 9 Streamlines at 25% rotor span at several moments in the case with S_H/S_{SS} =0.00

Combining Fig.8 and Fig.9, it can be seen that the high film cooling efficiency zone on the pressure side lasts from about t=0.3T to t=0.9T. During that time, the coolant is wrapped by the low energy wake flow of the vane after being ejected from film holes and then transports downstream along the pressure side of rotor blade. To some extent, that phenomenon enhances the film cooling performance. As a result, a high film cooling efficiency zone boundary forms, marked with L2 in Fig.8. High film cooling efficiency zone on the suction side appears from about t=0.6T. From then on, the coolant begins to flow towards the suction side. At that moment, the nearby area located downstream of film holes is covered with coolant, which forms this high film cooling efficiency zone. As time goes on, that part of coolant travels downstream and covers more area of blade surface. That explains the formation mechanism of the boundary of high film cooling efficiency zone on the suction side, which is marked with L3. At the meantime, more and more coolant continues to flow towards the suction side so that the cooling performance becomes better and better. When the vane trailing edge shockwave reaches the suction side of rotor blade, the pressure on the blade surface downstream of point A increases, which causes the separation of coolant flow from blade surface and the decrease of film cooling efficiency. That effect does not disappear until point A moves past leading edge film holes. The line L1 describes how point A travels with time, which is also another boundary of high film cooling efficiency zone on the suction side.

Film cooling performance: cases S_H/S_{SS} =0.05

Fig.10 shows the distributions of film cooling efficiencies in the cases with S_H/S_{SS}=0.05. Both the condition of θ=90° and that of θ=30° are shown. As shown in Fig.10a, when coolant is ejected vertically, the whole level of film cooling efficiency is relatively low. The L1 boundary caused by the sweeping of shockwave still exists. However, the cooling efficiency gradient across the shockwave becomes obviously lower. In addition, compared with the case in which film holes are located at the leading edge, the distribution of cooling efficiency is relatively uniform. However, in oblique coolant ejection case, as shown in Fig.10b, film cooling efficiency is significantly higher. The L1 boundary is not so obvious as that in Fig.10a. The cooling efficiency gradient across the shockwave is also not so large as that in Fig.10a. Coolant can also maintain a relative high coverage rate after flowing past shockwave.

Fig.11 shows the streamlines at several moments at 25% span in the case with S_H/S_{SS}=0.05 and θ=90°. It can be seen that there is a low film cooling efficiency zone near the film holes, which starts from about t=0.5T and lasts to about t=0.6T, as shown in Fig.11a, 11b and 11c. As time goes on, the region with low film cooling efficiency spreads downstream. That process forms the low film cooling efficiency boundary, denoted as L4 in Fig.10a. This zone has a significant effect on film cooling performance. According to Fig.11a, at t=0.5T, it can be ob-

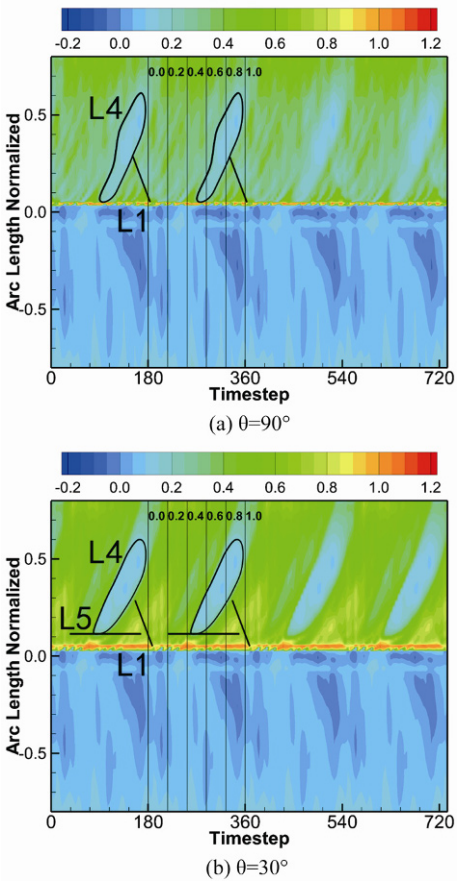

(a) θ=90°

(b) θ=30°

Fig. 10 Cooling efficiency contours at 25% rotor span in case with S_H/S_{SS} =0.05

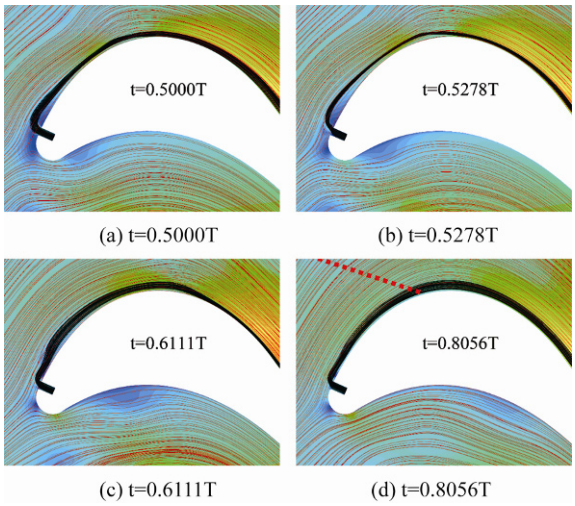

(a) t=0.5000T (b) t=0.5278T

(c) t=0.6111T (d) t=0.8056T

Fig. 11 Streamline of 25% rotor span at several moments in case with S_H/S_{SS} =0.05 and θ=90°

served that the film hole is covered by low energy wake flow. Therefore, the coolant flow cannot cover blade surface, which results in a low cooling efficiency near the exit of film holes. From then on to the moment of t=0.5278T, a portion of the low energy fluid continues to flow downstream along the blade suction side, and the streamwise size of influenced area becomes larger. At the moment of t=0.8056T, the rotor blade suction side begins to be affected by the vane trailing edge shockwave. The red dashed line in Fig.11d represents for the approximate location of shockwave. At t=1.0T, the zone with low cooling efficiency nearly vanishes.

Fig.12 shows the streamlines at 25% span in the case with S_H/S_{SS}=0.05 and θ=30°, and the moments shown here are all the same as that in Fig.11. Because the film hole axis is inclined to the blade surface, as shown in Fig.12a, it is relatively hard for coolant ejected from film holes to separate from blade surface, even being affected by the sweeping low energy vane wake flow. The low energy fluid continues to affect the film cooling efficiency on downstream blade surface with time goes on and that forms the low cooling efficiency zone surrounded by curve L4 in Fig.10b, although the coolant streamlines do not significantly separate from blade surface. In addition, as the oblique coolant jet flow is relatively harder to separate from blade surface, the low cooling efficiency zone surrounded by L4 does not start at $0.05S_{SS}$ as it is in the case with θ=90°. Instead, it begins at the location which is a little downstream of the film holes, as shown in Fig.10b by line L5.

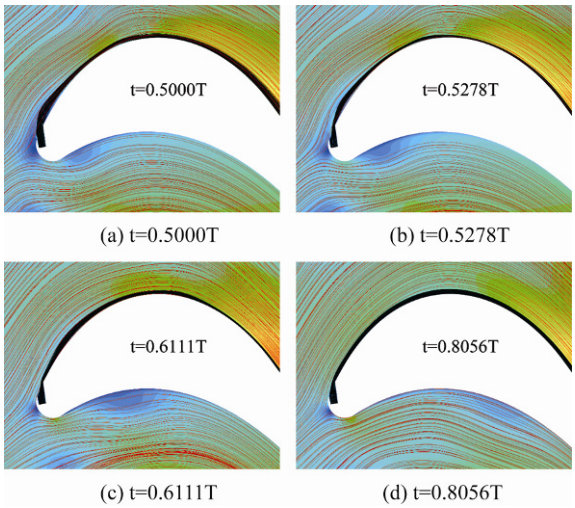

Fig. 12 Streamline of 25% rotor span at several moments in case with S_H/S_{SS} =0.05 and θ=30°

The unsteady sweeping of the shockwave at trailing edge affects not only the streamwise distribution of film cooling efficiency but also the spanwise distribution of that. Fig.13 shows the cooling efficiency contour on suction side in cases with S_H/S_{SS}=0.05. The red dashed lines represent for the approximate positions of point A at certain moments. In vertical coolant ejection case, as shown in Fig.13a, the coolant will mixed with main flow after being ejected out from the film holes. At the next moment, it will change its flow direction and then forms a pair of kidney eddies. After that the coolant flow will reattach to the suction side of rotor blade. Vane trailing edge shockwave began to reach rotor blade surface at about t=0.8056T. Because the shockwave is relatively far from film holes at this moment, its influences on suction side cooling performance are not obvious. When it comes to the moment of t=0.8889T, the shockwave causes a slight coolant separation which nearly splits the reattaching zone in half. At t=0.9444T the shockwave continues to move upstream. Coolant-reattaching region is influenced by shockwave and then is pushed upstream. The spanwise size of the zone with high cooling efficiency is also relatively larger than that at the moment of t=0.8889T. An obvious low cooling efficiency region appears downstream of the shockwave. At this moment, the intensity of shockwave near blade surface is relatively high, which causes the size of coolant separation zone to be larger. At t=1.0000T, the shockwave is very close to film holes. Coolant jet flow is pushed back to blade surface as soon as it is ejected out from the film holes. Then, under the effects of shockwave, coolant jet flow experiences separation and reattachment.

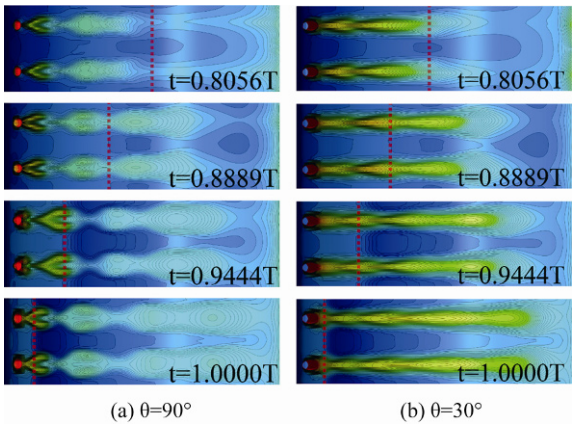

Fig. 13 Cooling efficiencies on suction side of rotor blade in cases with S_H/S_{SS}=0.05

The distribution of cooling efficiency is different when coolant is ejected obliquely, as shown in Fig.13b. Generally speaking, the coolant covers blade surface well and cooling efficiency is higher than that in the case with θ=90°. At t=0.8056T, it can be seen that the spanwise size of high film cooling efficiency region in the case with θ=30° is smaller than that in the case with θ=90°. However, the separation region and reattachment one both have longer sizes than those in θ=90° case. At t=0.8889T,

vane trailing edge shockwave has already affected the distribution of cooling efficiency. Because oblique coolant ejection has a stronger ability to resist flow separation, its influences on the reattachment zone are not so serious as that in the case with θ=90°. From t=0.8889T to t=0.9444T, the separation region and the reattachment one are both pushed upstream along the blade surface, but the spanwise size of high cooling efficiency zone hardly changes.

Film cooling performance: cases S_H/S_{SS} =0.10

Fig.14 shows the distributions of cooling efficiencies in the cases with S_H/S_{SS}=0.10. Because film holes in these cases are located downstream of the positions where they are in the cases with S_H/S_{SS}=0.05, area of the zone in which cooling efficiency is influenced by shockwave is surely smaller. According to Fig.14a, it can be seen that the cooling efficiency on blade surface near the leading edge is generally higher than that in the case with S_H/S_{SS}=0.05 and θ=30°. In addition, because the distance that the wake flow travels is longer, the wake flow decays more severely. Therefore, the effects of wake flow on this row of film holes decrease. Similarly, the sweeping vane trailing edge shockwave is also weaker when it arrives at the film holes. On the whole, cooling performances in the cases where film holes are located at $0.10S_{SS}$ suffer less from the sweeping shockwave and wake flow than that in other cases.

Furthermore, when the coolant is obliquely ejected, as shown in Fig.14b, the cooling efficiency on the suction side of rotor blade is even higher than that in the case as shown in Fig.14a. In the nearby region located downstream of the film cooling holes, the cooling efficiency in oblique ejecting case is significantly higher than that in vertical ejecting case. Moreover, the shockwave in Fig.14b has less impact on cooling performance than that in Fig.14a, which is for the reason that the reduction of cooling performance in this case is mainly caused by coolant flow separation. However, compared to vertical coolant jet flow, the oblique one has a natural resistance of flow separation. That makes for better film cooling performances in oblique coolant ejection cases.

Based on Fig.14b, it can be observed that the distance between low cooling efficiency zone surrounded by curve L4 and film cooling holes is more than $0.10S_{SS}$, which is farther than that in the case with S_H/S_{SS}=0.05 and θ=30°, as shown in Fig.10b. Comparing Fig.14b with Fig.14a, it can be seen that the low cooling efficiency zone caused by low energy wake flow is relatively more integrated in the case of oblique ejection. However, the low cooling efficiency zone mentioned above is scattered in the case of vertical ejection.

Fig.15 shows the vorticity contours at several moments near film holes at 25% rotor span in the cases with

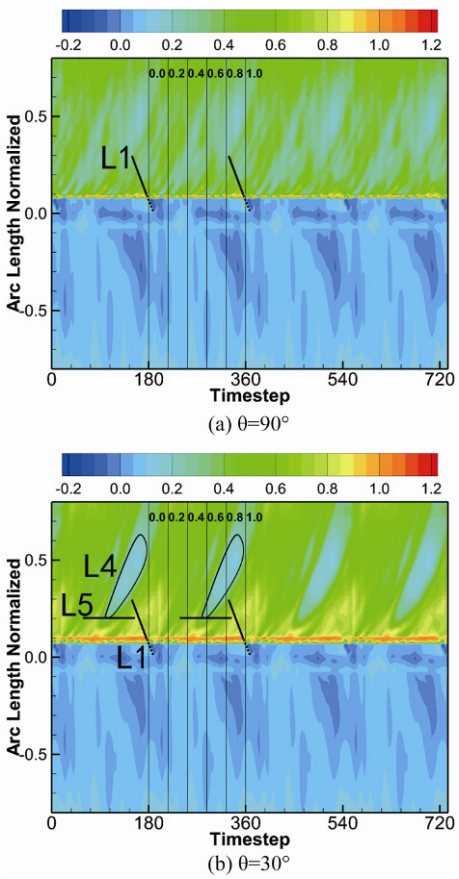

Fig. 14 Cooling efficiency contours at 25% rotor span in cases with S_H/S_{SS} =0.10

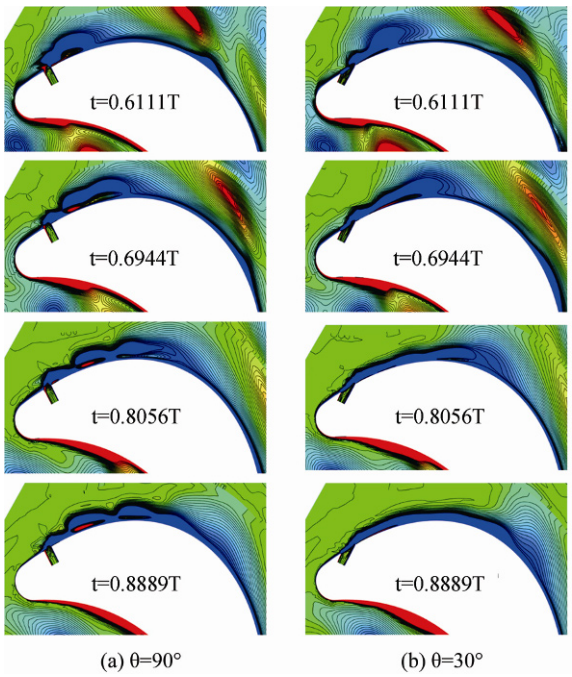

Fig. 15 Vorticity contours near film holes at 25% rotor span in cases with S_H/S_{SS}=0.10

S_H/S_{SS}=0.10. In these figures, it can be seen that the low energy wake flow is cut into several parts by vertically ejected coolant when the wake flow goes across film holes. Therefore, as time goes on, an integrated fluid cell with low energy is split into several small fluid cells. Each of these small fluid cells with low energy has an effect on film cooling performance of blade surface. Since these fluid cells are scattered, the distribution of cooling efficiency on blade surface is not continuous, as shown in Fig.14a. When it comes to the case of oblique coolant ejection, as shown in Fig.15b, the ejection angle of coolant is so low that the coolant flow cannot split the low energy wake flow. As a result, the low energy wake flow remains as an integrated fluid cell. However, the coolant flow gradually joins into the fluid cell and then flows along blade surface with time elapsing. Therefore, the low cooling efficiency zone shown in Fig.14b remains integrated.

Film cooling performance: cases S_H/S_{SS} =0.20

Fig.16 shows the variations of cooling efficiency with timestep and position in the cases with S_H/S_{SS}=0.20. According to Fig.16a, we can see that the influences of the vane trailing edge shockwave and wake flow on suction side film cooling efficiency become even less obvious. The space and time distribution of film cooling efficiency on blade surface downstream of film holes gets uniform.

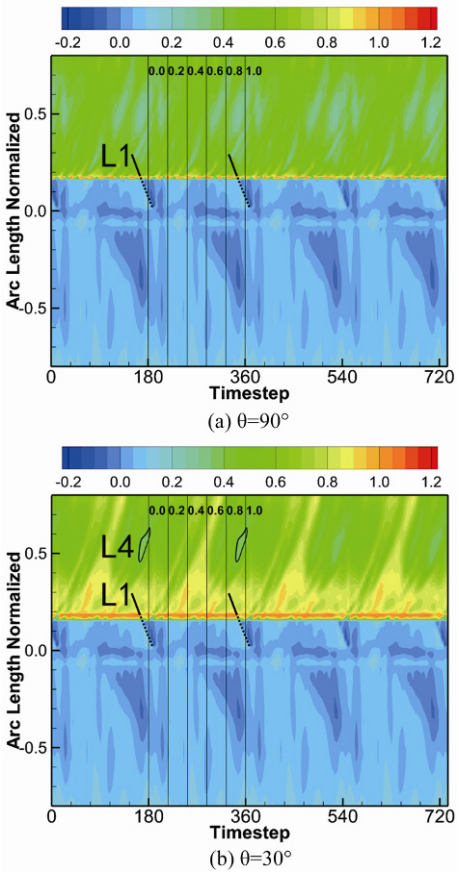

Fig. 16 Cooling efficiency contours at 25% span of rotor in cases with S_H/S_{SS} =0.20

Comparing Fig.16a with Fig.16b, it can be observed that the cooling performance in the case of oblique coolant ejection is significantly better. That is because the vane trailing edge shockwave needs to travel a relatively long distance to reach the film holes and the oblique coolant ejection has a strong ability to resist flow separation.

Time averaged film cooling efficiencies

According to the analysis mentioned above, it is easy to see that the film cooling performance of oblique coolant ejection is better than that of vertical coolant ejection, although it suffered more from the wake flow of vane. Table 4 shows time-averaged cooling efficiencies at different positions downstream of film holes in varying cases. Except for the case in which film holes are located at leading edge, all of the remaining cases are shown in this table. In each case, four monitoring positions are chosen to compare the differences of film cooling efficiency in varying cases, and they are respectively located $0.05S_{SS}$, $0.10S_{SS}$, $0.15S_{SS}$ and $0.20S_{SS}$ downstream of film hole central point.

Table 4 Time averaged cooling efficiency downstream film holes in different cases

Case	Position	$0.05S_{SS}$	$0.10S_{SS}$	$0.15S_{SS}$	$0.20S_{SS}$
0.05	straight	0.3182	0.2837	0.2758	0.2809
	oblique	0.6522	0.5600	0.5148	0.4783
0.10	straight	0.4172	0.3606	0.3466	0.3439
	oblique	0.7305	0.6583	0.5986	0.5393
0.15	straight	0.5454	0.5402	0.5226	0.4867
	oblique	0.8031	0.8016	0.7649	0.6913
0.20	straight	0.4973	0.4654	0.4533	0.4338
	oblique	0.8310	0.8212	0.7594	0.6858

As shown in Table 4, the cooling efficiencies in the cases of oblique coolant ejection are significantly higher than those in the cases of vertical ones at the locations which have the same distances downstream of the film holes. At the position which is $0.05S_{SS}$ downstream of the film holes, cooling efficiencies in oblique ejecting cases are at least 0.3 higher than those in vertical cases. That phenomenon approximately lasts to $0.10S_{SS}$ downstream of the film holes. At $0.20S_{SS}$ downstream of the film holes, the cooling efficiency in oblique ejecting cases are still significantly higher. Although the cooling efficiency decay rates in oblique ejecting cases are relative higher,

they can still maintain relatively better coolant coverages in a certain distance downstream of the film holes.

Conclusion

In this study, nine high load transonic air cooling turbine stage with different rotor blade film hole positions and oblique angles have been researched by unsteady numerical simulation. In those cases, both inner-extending trailing shockwaves and outer ones can be obviously observed. The periodically sweeping shockwave can result in flow separation on blade surface, which will affect the cooling performance on rotor blade. Here shows the conclusions acquired from this article.

1. The distributions of film cooling efficiency in steady simulation results are significantly different from that in time averaged unsteady ones. Besides the general differences in numerical values, there are also difference existing in streamwise and spanwise cooling efficiency distribution characteristics. Sweeping vane trailing edge shockwave does affect film cooling performance on rotor blade significantly.

2. In the turbine stage investigated in this article, the vane trailing edge outer-extending shockwave can reach the suction side of rotor blade at certain moments. Those moments start from about t=0.8T and last to about t=1.0T. In that twenty percent of a period, coolant near the leading edge will separate from rotor blade. Film cooling performance on suction side of rotor blade is periodically affected by sweeping shockwave.

3. With the distance between the film holes and the leading edge of rotor blade being larger, the coolant will suffer less from the sweeping vane trailing edge shockwave. In the case that film holes are located at leading edge, the time during which cooling performance is affected by sweeping shockwave is about one fifth of a period. That time decreases with the film holes moving downstream. In the cases that film holes are situated at 0.20 times of the blade profile curve length, that time decreases to only about ten percent of a period.

4. When the film holes are located at the same streamwise position, the cases that oblique coolant ejections suffer less from the sweeping shockwave than that of vertical ones. At 0.05 times of the blade profile curve length downstream of film holes, the time-averaged film cooling efficiencies in the cases of oblique ejections are at least 0.3 higher than those in the vertical ejection cases. Within 0.20 times of the blade profile curve length downstream of film holes, oblique coolant ejection can also maintain more than 0.2 film cooling efficiency advantage. However, the oblique coolant jet flow will not split the low energy fluid from vane wake flow into pieces, which affects rotor blade film cooling performance.

5. Vane trailing edge shockwave can also affect the spanwise distribution of cooling efficiency on blade surface. Shockwave can push the coolant flow structure to move upstream and the affected region will be wider in spanwise direction. Compared to the cases of vertical coolant ejections, the cases of oblique ones have narrower affected regions. However, the coolant flow structures in those cases do not change a lot. The affected regions in the cases of oblique coolant ejections suffer less from the sweeping shockwave at the trailing edge of vane.

Overall, in high-load transonic turbine stages, the unsteady sweeping vane trailing edge outer-extending shockwave can definitely affect film cooling performance on suction side of rotor blade near leading edge for a quite long portion of a period. The sweeping shockwave can decrease the film cooling efficiency located downstream of it by causing coolant flow separation. Film holes far from leading edge of rotor blade suffer less from the sweeping shockwave. Oblique coolant ejection has a better film cooling performance under the sweeping of shockwave, which reflects in a lower film cooling efficiency decay across shockwave and a smaller change in coolant flow structure.

Acknowledgments

The authors thank all the professors at Engine Dynamics Research Center of Harbin Institute of Technology for their support, encouragement, constructive suggestions and assistances. The author would also like to thank the support of the National Natural Science Foundation of China (NSFC), Grant No. 51421063.

References

[1] HUANG Weiguang, CHEN Naixing, Nobuhiko YAMASAKI, et al. Numerical Simulations on Unsteady Rotor-Stator Interaction in Turbine Cascades[J]. Journal of Engineering Thermophysics, 1999, 20(3): 294−298.

[2] Brachmanski R E, Niehuis R, Bosco A. Investigation of a Separated Boundary Layer and its Influence on Secondary Flow of a Transonic Turbine Profile[C]//ASME Turbo Expo 2014: Turbine Technical Conference and Exposition. American Society of Mechanical Engineers, 2014: V02CT38A022-V02CT38A022. Düsseldorf, Germany.

[3] Ochs M, Schulz A, Bauer H J. Investigation of the Influence of Trailing Edge Shock Waves on Film Cooling Performance of Gas Turbine Airfoils[C]. ASME Turbo Expo Power for Land Sea & Air, Montreal, Canada, 2007: 465−474.

[4] Adami P, Montomoli F, Belardini E, et al. Interaction Between Wake and Film Cooling Jets: Numerical Analysis[C]// American Society of Mechanical Engineers, 2004:

1053−1063. Vienna, Austria.

[5] Ou S, Han J C, Mehendale A B, et al. Unsteady Wake Over a Linear Turbine Blade Cascade With Air and CO_2 Film Injection: Part I: Effect on Heat Transfer Coefficients[J]. Journal of Turbomachinery, 1994, 116(4): V03AT15A061.

[6] MEHENDALE, A. B, HAN, J.C.et al. Unsteady wake over a linear turbine blade cascade with air and CO_2 film injection. II: Effect on film effectiveness and heat transfer distributions[J]. Journal of Turbomachinery, 1994, 116(4): V002T08A013.

[7] LI Hongyang, ZHENG Yun. Effect of Rotor-Stator Interaction on Film-Cooling of Turbine Blade [J]. Journal of Beijing University of Aeronautics and Astronautics, 2016, 42(1): 139−146.

[8] Rigby M J, Johnson A B, Oldfield M L G. Gas Turbine Rotor Blade Film Cooling with and without Simulated NGV Shock Waves and Wakes[C]// ASME, 35th International Gas Turbine and Aeroengine Congress and Exposition, 1990. New York, USA.

[9] ZHOU Yong, ZHAO Xiaolu, XU Jianzhong. Numerical Simulation of the Unsteady Effect of Upstream Shocks on Film-Cooling in a 1+1/2 Turbine Stage[J]. Journal of Engineering Thermophysics, 2007, 28(6): 933−935.

[10] CHI Zhongran. Heat Transfering Design for Air-Cooled Turbine Blades[D]. Harbin: Harbin Institute of Technology, 2010: 107−110.

[11] CHI Z, REN J, JIANG H. Coupled Aerothermodynamics Optimization for the Cooling System of a Turbine Vane [J]. Journal of Turbomachinery, 2014, 136(5): 051008.

[12] CHI Z, REN J, JIANG H. Cooling Structure Optimization for a Rib-Roughed Channel in a Turbine Rotor Blade [C]//ASME Turbo Expo 2013: Turbine Technical Conference and Exposition. American Society of Mechanical Engineers, 2013: V03BT11A009-V03BT11A009. San Antonio, USA.

[13] CHI Z, WANG S, REN J, et al. Multi-Dimensional Platform for Cooling Design of Air-Cooled Turbine Blades [C]//ASME Turbo Expo 2012: Turbine Technical Conference and Exposition. American Society of Mechanical Engineers, 2012: 207−218. Copenhagen, Denmark.

[14] Benabed M, Azzi A, Jubran B A. Numerical Investigation of the Influence of Incidence Angle on Asymmetrical Turbine Blade Model Showerhead Film Cooling Effectiveness[J]. Heat and Mass Transfer, 2010, 46(8): 811−819.

[15] Sridhar M, Sunnam S, Goswami S, et al. CFD Aerodynamic Performance Validation of a Two-Stage High Pressure Turbine[C]// ASME 2011 Turbo Expo: Turbine Technical Conference and Exposition. 2011: 1175−1184. Vancouver, Canada.

[16] MARTELLI F, ADAMI P. Unsteady Aerodynamics and Heat Transfer in Transonic Turbine Stages Modelling Approaches[C]// 8th International Congress of Fluid Dyanmics & Propulsion，2006: 14-17．Sharm El-Shiekh, Egypt.

[17] Akin M B, Sanz W. The Influence of Transition on CFD Calculations of a Two-Stage Counter-Rotating Turbine [R]. ASME Paper 2014-GT-26044, 2014. Düsseldorf, Germany.

[18] ZHOU L, WEI W, CAI Y H. Effect of Unsteady Wake Transportation on Film Cooling Flowfield of Rotating Turbine Blade[J]. Journal of Aerospace Power, 2012, 27(8): 1696−1703.

[19] Narzary D P, Gao Z, Mhetras S, et al. Effect of Unsteady Wake on Film-Cooling Effectiveness Distribution on a Gas Turbine Blade with Compound Shaped Holes[C]// ASME Turbo Expo 2007: Power for Land, Sea, and Air. American Society of Mechanical Engineers, 2007: 79−91. Montreal, Canada.